◆ Human Brain Mapping 13:226–238(2001) ◆

Early Discrimination of Coherent versus Incoherent Motion by Multiunit and Synaptic Activity in Human Putative MT+

Istvan Ulbert,[3,4] George Karmos,[3] Gary Heit,[4] and Eric Halgren[1,2]*

[1]*Massachusetts General Hospital NMR Center, Harvard Medical School, Charlestown, Massachusetts*
[2]*INSERM E9926, Marseilles, France*
[3]*Institute for Psychology, Hungarian Academy of Sciences, Budapest, Hungary*
[4]*Department of Neurosurgery, Stanford University, Stanford, California*

Abstract: A laminar probe was chronically implanted in human putative MT+. The area was specifically responsive to globally coherent visual motion, a crucial aspect of the perception of movement through space. The probe contained 23 microcontacts spaced every 175μ in a linear array roughly perpendicular to the cortical surface. Current-source density (CSD) and multiunit activity (MUA) were recorded while viewing initially stationary random dot patterns that either moved incoherently or dilated from the central fixation. Onset of visual motion evoked large MUA/CSD activity, with coherent motion evoking earlier and faster-rising MUA/CSD activity than incoherent, in both superficial and deep pyramidal layers. The selective response, peaking at ≈115 ms, was especially large in deep pyramids, providing evidence that information necessary for visual flow calculations is projected from MT+ at an early latency to distant structures. The early onset of differential MUA/CSD implies that the selectivity of this area does not depend on recurrent inhibition or other intrinsic circuitry to detect coherent motion. The initially greater increase of MUA to coherent stimuli was followed by a greater decrease beginning at ≈133 ms, apparently because of recurrent inhibition. This resulted in the total MUA being greater to incoherent than coherent stimuli, whereas total rectified CSD was overall greater to coherent than to incoherent stimuli. However, MUA distinguished stationary from moving stimuli more strongly than did CSD. Thus, while estimates of total cell firing (MUA), and of total synaptic activity (CSD) generally correspond to previously reported BOLD results, they may differ in important details. *Hum. Brain Mapping 13:226–238, 2001.*

Key words: cerebral cortex; neocortex; occipital lobe; visual cortex; electroencephalography; vision; evoked potentials; visual perception; motion perception

INTRODUCTION

In the human, moving visual stimuli have been found to evoke specific hemodynamic activation in a small area at the dorsolateral occipitotemporal junction, using positron emission tomography (PET) [Watson et al., 1993] and functional magnetic resonance imaging (fMRI) [Tootell et al., 1995; Beauchamp et al., 1997]. This area is termed MT+ because it ap-

Contract grant sponsors: Human Frontiers Science Program Organization (RG0025/1996), National Institutes of Health (NS 18741), National Foundation for Functional Brain Imaging (DOE grant DE-FG03-99ER62764), and Office of Naval Research.

Received for publication 4 February 2000; Accepted 30 March 2001.

*Correspondence to: Eric Halgren, Ph.D., MGH-NMR Center, Rm. 2301, Bldg. 149, 13th St., Charlestown, MA 02129.
E-mail: halgren@nmr.mgh.harvard.edu

pears to be homologous to area MT (or V5) in the monkey, plus the adjacent smaller area MST. Neurons in monkey MT fire specifically to moving visual stimuli [Maunsell and VanEssen, 1983]. Anatomically, MSTd follows MT in the dorsal visual processing stream [Ungerleider and Desimone, 1986; Boussaoud et al., 1990], and its cells also respond to moving visual stimuli. However, compared to MT, MSTd neurons are especially sensitive to the coherence of visual motion [Tanaka et al., 1986; Duffy and Wurtz, 1991; Graziano et al., 1994; Geesaman et al., 1997]. For example, a set of dots that suddenly start expanding radially outward evokes much greater activity than would a set of dots in the same locations that begin to move at the same velocity and average direction but at random orientations to the radial [Albright, 1989; Tanaka et al., 1989; Lagae et al., 1994]. Radial motion of visual stimuli commonly happens when we move through space, looking ahead, and is termed "optic flow." The responsiveness of MSTd to such patterns suggests that it may assist in visual navigation by calculating the direction of heading with respect to the direction of gaze [Lappe and Duffy, 1999; Andersen et al., 2000].

This possibility has been elaborated in quantitative models in which MSTd calculates optic flow by combining inputs from MT, which is posited to detect local motion [Lappe et al., 1996; Perrone and Stone, 1998]. For example, several MT cells, each sensitive to local retinal movement away from a given point, are hypothesized to converge on a particular MSTd cell that would then fire selectively when the animal moves toward that location. Under this model, the net synaptic activity to coherent vs. incoherent motion could be the same, but increased convergence to coherent stimuli would result in an increased initial multiunit response. An alternative hypothesis notes that, although MT shows much less selectivity for coherent stimuli than MSTd, some MT cells do exhibit that property [Lagae et al., 1994]. This raises the possibility that such cells selectively project to MSTd, and thus that selectivity for coherent motion may be present in synaptic as well as multiunit activity from the earliest onset of excitation.

In a third model, the sensitivity to global motion would be produced by using reciprocal inhibition to integrate local motion with location. In MT, cells excited by motion in a particular direction and location tend to be inhibited by movements in other directions in surrounding locations [Bradley and Andersen, 1998]. In an expanding dot pattern, dots that share receptive fields would tend to move in the same directions, and thus would inhibit each other less than if they were moving randomly with respect to each other, thus explaining the larger MSTd activation to coherently moving stimuli. Note that in this model, coherent and incoherent stimuli would initially activate MSTd cells equally, and the responses to incoherent stimuli would then be attenuated by inhibition via an interpolated interneuron after a delay.

In the current study, we attempted to distinguish between these alternative models by measuring neuronal activity from putative human MT+ during coherent vs. incoherent motion. PET and fMRI are not able to resolve this issue because they integrate neural activity over 1–60s, and thus cannot resolve the onset of activation. Furthermore, PET and fMRI integrate activation over 3–8 mm, and thus do not resolve different cortical layers. Finally, because PET and fMRI appear to measure a consequence of energy consumption, they do not distinguish between synaptic currents and neuronal action potentials. Laminar recordings from multiple closely spaced microcontacts have been used to characterize the synaptic currents and action potentials underlying cortical processing in animals [Mitzdorf, 1985; Schroeder et al., 1998; Sukov and Barth, 1998]. We believe that this report is the first use of laminar recordings during behavioral testing in a human. It was found that the selective activation by coherent stimuli in putative human MT+ is present from its earliest activation. The laminar technique may also be applied profitably to studying the synaptic bases of other types of cognitive processing in humans.

METHODS

Subject

The subject was a 41-year-old right-handed woman of normal intelligence and personality with a 25-year history of medically intractable complex partial seizures. She participated after fully informed consent, monitored by the Stanford IRB and according to NIH guidelines conforming to the Declaration of Helsinki. Spontaneous seizures began with an aura of spatial distortion of the room and/or distortions of observed faces. MRI was normal. An incidental finding of the intracarotid sodium amytal (Wada) test was a left peri-clinoid internal carotid artery aneurysm, which was embolized with an endovascular coil. Ictal SPECT showed increased uptake in the right temporal region, and scalp EEG at ictal onset was localized to the right occipito-temporal region. On the basis of these data, surgical therapy was planned to involve the right occipito-temporal junction. As an aid to definition of the margins of the resection, a subdural grid and two

subdural strips were implanted in the region of the focus for 4 days (Fig. 1A). Intracranial EEG of spontaneous seizure onset, supplemented by intraoperative ECOG, permitted a tailored resection of the right occipito-temporal area. The patient remains seizure-free at 12-month follow-up. No abnormalities were observed in the pathology specimen.

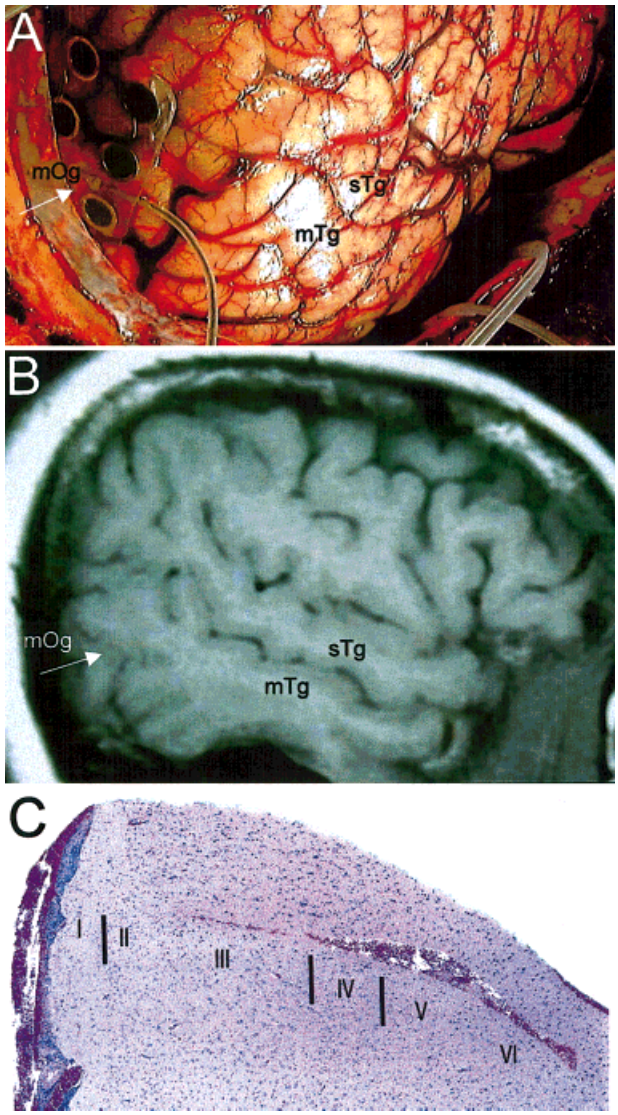

Figure 1.
Location of laminar probes. **A.** Intraoperative photograph showing placement of the laminar probe (arrow) underneath the subdural grid of macrocontacts, at the lateral occipito-temporal junction. The laminar probe is in the middle occipital gyrus (mOg), just posterior to the middle temporal gyrus (mTg). mTg is identified in relation to the superior temporal gyrus (sTg). **B.** Sagittal preoperative MRI showing the laminar probe's location (arrow) in the lip of the lateral occipital sulcus, near its intersection with an ascending branch of the inferior temporal sulcus (corresponding to the anterior occipital sulcus). **C.** Photomicrograph of the electrode track, with lines separating layers I/II, III/IV, and IV/V. Luxol fast blue.

Electrodes

A laminar electrode was placed under visual observation in a location within the planned resection. The electrode consisted of a 400μ diameter polyimide tube with twenty-three 40μ diameter 90%Pt–10%Ir contacts spaced at 175μ center-to-center, arrayed in a line perpendicular to the cortical surface. In gross anatomical terms, the laminar probe was located in the lip of the lateral occipital sulcus, near its intersection with the inferior temporal sulcus (Fig. 1B). In Talairach [1988] coordinates, the laminar probe was located at +50 (right), −60 (posterior) +3 (up). This is 9–16 mm anterior to the center of motion-selective activation previously found for human MT+ using PET (42,−69,0) [Watson et al., 1993] and fMRI (45,−76,3) [Tootell et al., 1995]. In these studies, the center of activation had a standard deviation of about 8 mm in the anterior-posterior dimension, and the entire MT+ activation was about 10–15 mm in each dimension. Thus, the laminar probe appeared to be located at the anterior edge of MT+, i.e., in the proposed location of MSTd. Because MT neurons may also display a preference for globally coherent motion, it is possible that the electrode was located in MT. Thus, we will refer to the probe location as MT+, and the conclusions should be construed as referring to how sensitivity to coherent motion arises within this general area.

The cortical tissue surrounding the electrode was removed en bloc at the definitive surgery. Alternate sections were stained with luxol fast blue, Bielschowsky, and haematoxilin and eosin, in order to identify cortical laminae using standard criteria (Fig. 1C). A silastic disk was attached to the top of the laminar probe. This disk was held against the pial surface by the subdural grid, thus fixing mechanically the distance from the pial surface to the first contact, and allowing the microcontacts to be approximately located with respect to cortical lamina.

Recordings

Differential recordings were made from 22 pairs of successive contacts. After wideband (DC-10,000 Hz) preamplification (gain 10×, CMRR 90db, input impedance 10^{12} ohms), the signal was split into field potentials (filtered at 0.2–500 Hz, gain 1,000×, digitized at 1,000 Hz, 16 bit) and multiunit activity (MUA: filtered at 200–5,000 Hz, gain 1,000×, digitized at 10,000 Hz,

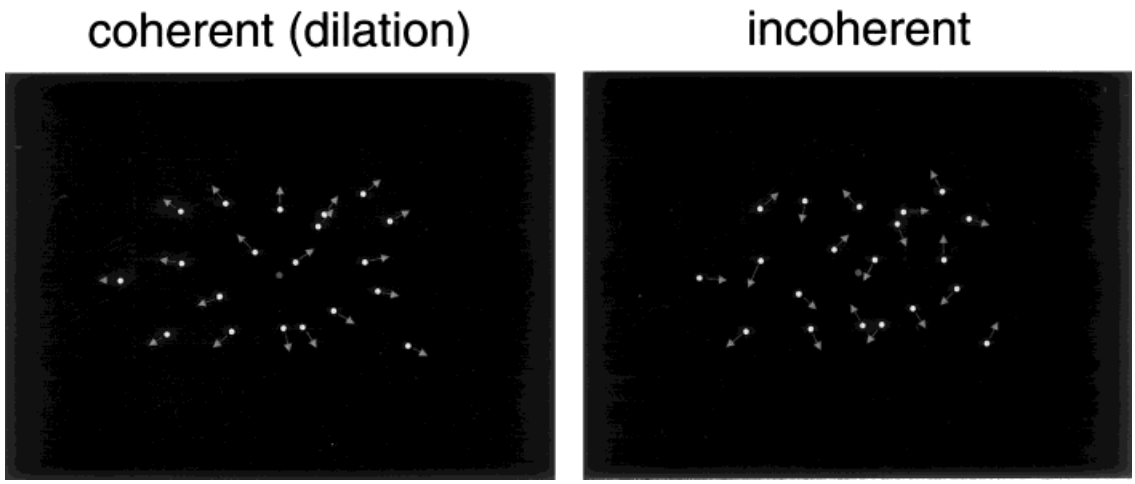

Figure 2.
Visual stimuli. Left. Randomly placed dots in the coherent stimuli moved radially away from the center of the display. Right. Dots in incoherent stimuli moved in random directions but with the same average starting points and directions.

12 bit), and stored continuously with stimulus markers.

Estimated current source densities (CSD) at electrode contacts 3–20 (j) were calculated as:

$$CSD_j = (.23(i_j - i_{j-1}) + .54(i_{j+1} - i_j) + .23(i_{j+2} - i_{j+1}))/h \quad (1)$$

where i_j is the estimated current between electrode contacts j and j-1, and h is the intercontact distance, 0.175 mm. The i_j are calculated from differences in the field potentials v (i.e., the output of a differential amplifier channel) divided by the interelectrode tissue resistance rh (equal to the resistance r, assumed to be homogeneous and equal to 20 ohms/mm [Nicholson and Freeman, 1975; Mitzdorf, 1985], multiplied by the intercontact distance):

$$i_j = (v_j - v_{j-1})/rh \quad (2)$$

Combining formula (1) and (2), one arrives at the standard five-point Hamming filter estimate for CSD [Rappelsberger et al., 1981]:

$$CSD_j = (.23v_{j-2} + .08v_{j-1} - .62v_j + .08v_{j+1} + .23v_{j+2})/rh^2 \quad (3)$$

CSD at electrode contacts 2 and 21 were calculated by applying the same formula after estimating the potentials at (pseudo-) contacts 0 and 23 using linear extrapolation [Vaknin et al., 1988]. MUA was obtained by further filtering (300–3,000 48 db/oct, zero phase shift) the signal in a range found to detect action-potentials in previous studies [Grover and Buchwald, 1970; Halgren et al., 1977; Legatt et al., 1980]. A continuous estimate of MUA was derived by rectifying, and then low-pass filtering (50 hz digital, 24 db/oct zero phase shift) the signal. The field potential gradient was also filtered (1–40 Hz, 24 db/oct zero phase shift), prior to calculating the CSD. Appropriate artifact rejection was performed using amplitude threshold criteria on field potential gradient and MUA. All steps of the analysis were performed using Neuroscan Edit 4.1.1 software (Neuroscan, Inc.). Details of electrode construction, recordings and analysis can be found in Ulbert et al. [2001].

Rationale of CSD/MUA analysis

CSD identifies possible synaptic generators using high-resolution maps of field potentials within the generating structure [Schroeder et al., 1998; Sukov and Barth, 1998]. The difference in potential between adjacent recording contacts is equal to the current flowing between them times the resistance. In cortical structures, current flows in the tangential direction can be assumed to be symmetrical (at least to the first approximation), and thus to cancel each other out. Consequently, changes in current in the radial dimension imply local passage of current across the neuronal membrane [Nicholson and Freeman, 1975]. EPSPs result from the passage of positive charge from the extracellular to the intracellular space, termed a *sink* in

CSD. Surrounding the sink are passive sources of current. In contrast, typical hyperpolarizing IPSPs result from active current sources, and are surrounded by passive sinks. Active and passive transmembrane current flows can be distinguished using simultaneous MUA. For example, an increase in MUA suggests that simultaneous sinks locate active excitatory synapses, and simultaneous sources locate passive return currents. The origin of these synapses may then be inferred from the known anatomical distribution of different pathways across cortical laminae. Although it is theoretically possible that axonal action potentials (especially in terminal arborizations), dendritic spikes, nonsynaptic active currents, and even glial currents could contribute to CSD measures; these sources are considered unlikely to contribute significantly in the current experimental protocol [for discussion, see Mitzdorf, 1985; Schroeder et al., 1995].

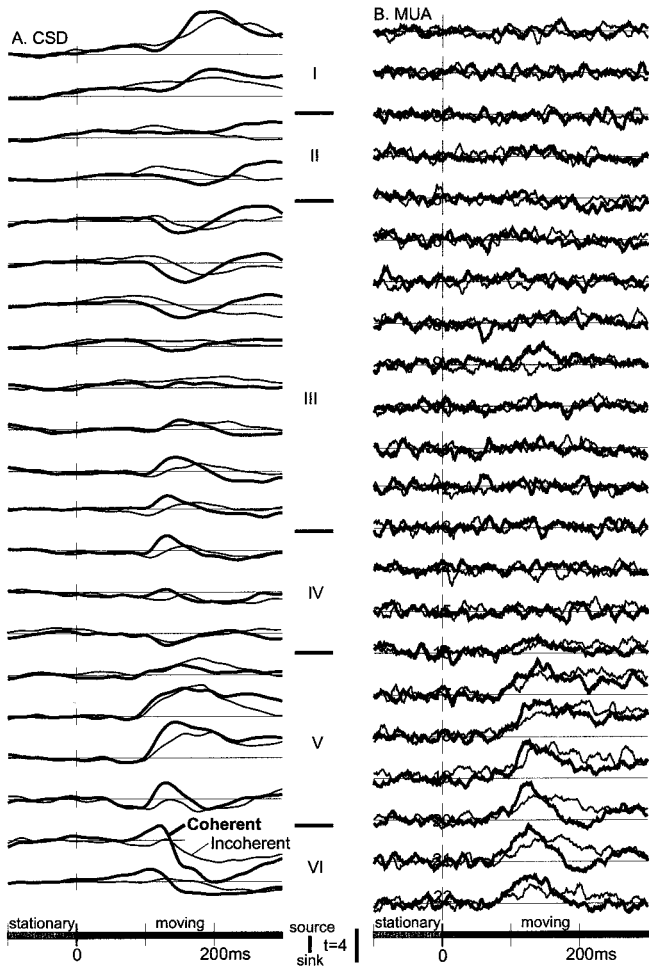

Figure 3.

Population synaptic and unit activity to moving and stationary random dot patterns **A.** Population synaptic activity is measured as current-source density (CSD) at 21 locations, separated by 175μ intervals, spanning the cortical laminae. Recordings are displayed with the most superficial location at top. Activation is earlier and stronger to coherently moving stimuli (thick lines) than to incoherently moving (thin lines). **B.** Population unit activity is measured as multiunit activity (MUA) from the same contacts. Again, coherent motion evokes a larger and earlier response, especially in the cortical layers containing superficial pyramids (level 9). The MUA response in the deep pyramidal layer tends to be biphasic to coherent stimuli and monophasic to incoherent. The vertical bar indicates a *t* value of 4.0, compared to baseline, corresponding to a $P < 0.0001$.

Coherent vs. incoherent motion

At the beginning of each trial, 20 white dots (each subtending 0.15° of visual angle) were randomly distributed on a black background in a region subtending 3.5° vertical by 7.0° horizontal (Fig. 2). Between trials, fixation was maintained on a white dot in the center of that region. After remaining stationary for 533 ms, the dots moved for 373 ms at 6.7°/sec and then remained stationary for another 533 ms. On the 160 trials with incoherent motion, the dots moved in random directions; on the 160 trials with coherent motion, the dots moved radially away from the center (i.e., the pattern dilated). The onsets of successive trials were separated by 3,500 ms. The subject was instructed to observe the stimuli attentively, and avoid moving her eyes or blinking during the trials.

Separate averages were made of single sweep CSD and single sweep MUA from trials with coherent vs. incoherent motion, after rejecting artifacts using an amplitude criterion. Statistical comparisons were made using data from the ≈120 individual trials remaining after artifact rejection. At each latency point, *t* tests (Neuroscan Edit 4.1.1) were used to compare trials with coherent motion to those with incoherent motion, as well as each condition to the baseline period. To provide protection against type 1 errors resulting from multiple comparisons across channels and latencies, an uncorrected statistical significance threshold of $P < 10^{-5}$ was used.

RESULTS

Response to stationary visual stimuli

The responses are presented as waveforms (Fig. 3) and as spatiotemporal color-coded maps (Fig. 4). Onset of the stationary visual pattern evoked a small but significant increase in MUA in the deep pyramidal layer, with an onset latency of ≈100 ms and peak latency of ≈140 ms (see red contour lines in channels

17–19 of Fig. 4D, beginning ≈400 ms prior to stimulus movement). Stationary patterns also evoked a CSD sink, in layer IV and a source-sink pair in the deep pyramidal layers V and VI (black-white contour lines, Fig. 4D). The deep MUA/CSD response beginning at ≈100 ms is followed by a strong superficial cortical CSD source that begins at ≈140 ms and peaks at ≈190 ms (black contours, channels 2–4, at –300 ms, Fig. 4D). Like the deep source, the superficial source is followed by a sink beginning at ≈370 ms peaking at ≈450 ms after stationary stimulus onset (white contours, channels 2–4, at –100 ms, Fig. 4D). The superficial CSD sink/source, as well as the deep sink/source, are not associated with significant changes in MUA (Fig. 4D). However, the total MUA across all layers shows a tendency to decrease during this period (Fig. 5A).

Response to coherent visual motion

The onset of visual motion by formerly stationary stimuli evoked a large MUA and CSD response, especially when the motion was coherent (Figs. 3–5). Again, the most prominent MUA response was located in the deep pyramidal layers, but a response was now also present in the superficial pyramidal layers.

Coherent visual motion evoked a strong MUA increase in the deep pyramidal layer, beginning at ≈110 ms, peaking at ≈120–150 ms, and persisting weakly throughout the period of stimulation (thick lines, channels 17–21, Fig. 3B, and red contours, Fig. 4A). Coherent motion also evoked a significant CSD sink in layer IV (white contours, Fig. 4A), surrounded by sources in layers III and V-VI (black contours, Fig. 4A). In addition, a later but prominent CSD sink is present in layer VI. This source-sink-source-sink pattern began at ≈105 ms, peaked at ≈140 ms, with portions of it persisting throughout the period of visual motion. The temporal association of increased MUA with the CSD sink indicates that the sink represents active excitatory population synaptic currents. The initial sink was centered in layer IV, followed by the layer VI sink.

Coherent visual motion also evoked a weak but significant MUA increase in the superficial pyramidal layer, peaking at ≈145 ms (red contours, channel 9, Fig. 4A). This firing was temporally correlated with a superficial layer III sink, surrounded by sources in layers I–II and deep layer III. These MUA and CSD responses in the superficial pyramidal layer were all transient, and did not persist beyond 200 ms after motion onset. Finally, coherent motion evoked a sustained source in layer I, beginning at ≈135 ms and continuing throughout the stimulation period (black contours, channels 1–3, Fig. 4A).

Comparison of phasic responses to coherent vs. incoherent motion

The overall pattern of the CSD/MUA response to incoherent motion was similar to that evoked by coherent, except that the phasic response was weaker and delayed, whereas the sustained response was more robust. These differences can be examined by comparing the thick (coherent) and thin (incoherent) lines in Figures 3A and 3B, by comparing Figure 4A (coherent) to 4B (incoherent), and by examining Figure 4C, which shows the pattern obtained by subtracting the CSD/MUA response to incoherent motion from that to coherent.

The decreased phasic response is seen most clearly in the deep pyramidal layer. Specifically, the deep pyramidal MUA increase to incoherent visual motion did not begin until ≈120 ms, and did not peak until ≈140–160 ms (red contours, channels 17–21, Fig. 4B). Similarly, the deep pyramidal layer source evoked by incoherent motion did not begin until ≈110 ms, and did not peak until ≈180 ms (black contours, channels 17–21, Fig. 4B). The direct comparison of deep pyramidal responses indicates that coherent motion evokes a larger CSD response beginning at ≈100 ms, and a larger MUA response beginning at ≈110 ms, with coherent/incoherent differences peaking at about 120 ms (channels 19–21, Fig. 4C).

The CSD/MUA response in the superficial pyramidal layer also appeared later and weaker to incoherent stimuli, at ≈200ms (MUA- red contours in channel 8; CSD source, black contours in channels 9–10; CSD sink, white contours in channels 6–8; Fig. 4B). Note that the superficial pyramidal MUA and CSD responses are consistently delayed from those in the deep pyramidal layers. However, the deep and superficial responses appear to be linked, in that when the deep response is weaker (i.e., between incoherent vs. coherent motion), the superficial response is also, and when the deep response is delayed (again, between incoherent vs. coherent motion), the superficial response is also.

Comparison of sustained responses to coherent vs. incoherent motion

In striking contrast to the decreased phasic response to incoherent as compared to coherent motion, the sustained MUA response was *greater* to *in*coherent motion. This is especially evident in channels 17–22, where initially (from ≈100–150 ms) the MUA activity is larger to coherent motion, and then (from ≈160–260 ms) the MUA activity is larger to coherent motion

(thick vs. thin lines; Fig. 3B, 4C). At ≈200 ms, for example, the firing of the deepest pyramids to coherent motion is seen to actually fall below baseline, whereas their firing to incoherent motion remains high.

At the same time that the deep pyramidal MUA is showing this increased sustained response to *incoherent* motion, the deep pyramidal CSD source/sink is unchanged or indeed (after ≈250 ms) is somewhat

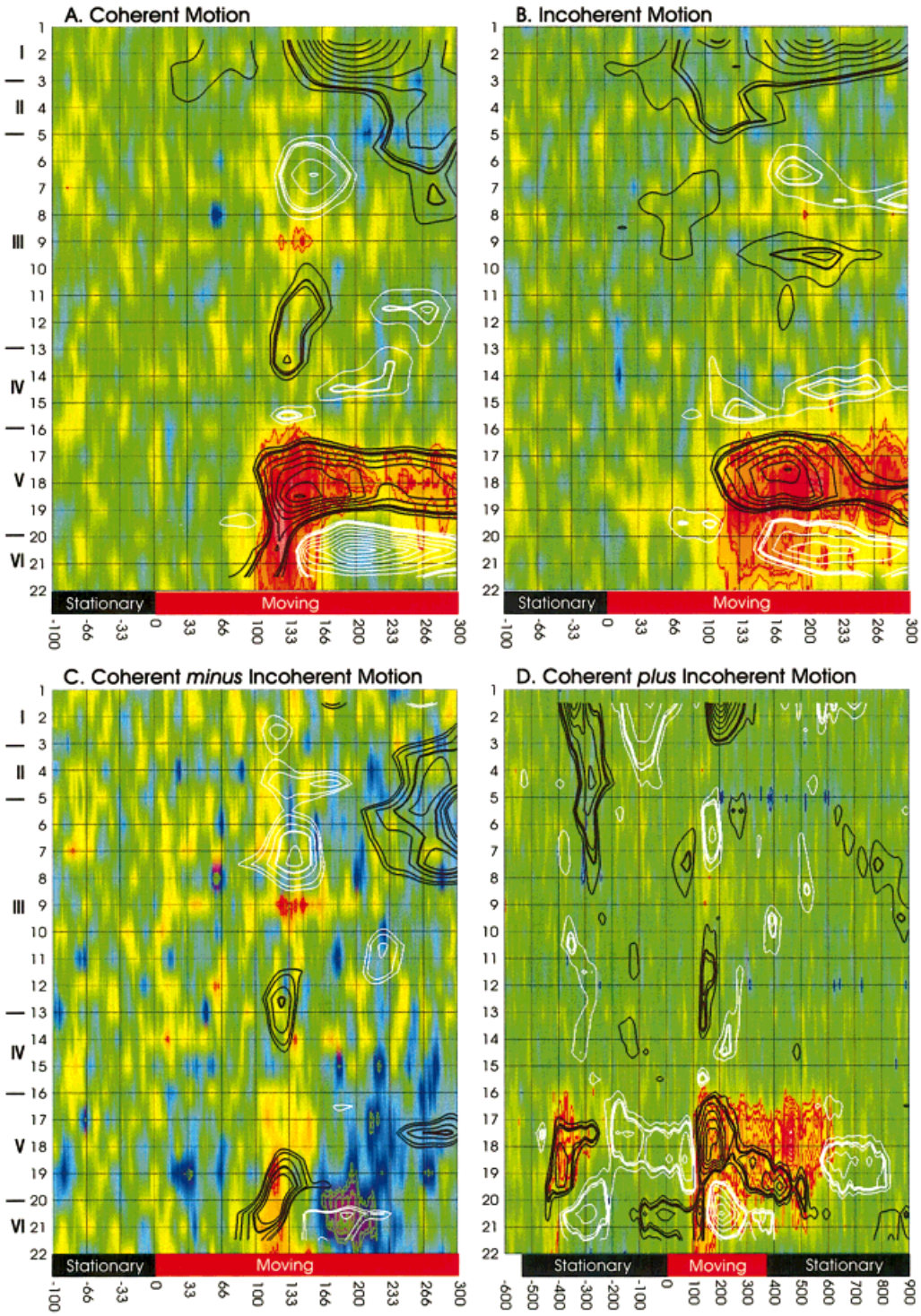

Figure 4.

larger to *coherent* motion. Yet, as noted above, the deep pyramidal CSD source/sink appears to represent the population EPSP that is causing the deep pyramidal MUA. This dissociation suggests that active inhibition may be present during this period, especially to coherent stimuli.

CSD/MUA responses integrated across cortical layers and time windows

To compare the current results with lower-resolution noninvasive hemodynamic measures, the CSD and MUA measures were combined across the recording sites. The CSD measure was rectified before summing in order to arrive at an estimate of total transsynaptic current flow (cf. the "AVREC" measure of Schroeder et al. [1995]). The resulting waveforms are shown in Figure 5A. Examination of these waveforms reveals the overall greater response of this area to moving vs. stationary stimuli and to coherent vs. incoherent motion. However, clear distinctions also are apparent. For example, the CSD response to stationary stimuli appears to be relatively large (gray arrow, Fig. 5-1A), as does the sustained MUA response to incoherently moving stimuli (black arrow, Fig. 5-2A). These points were examined quantitatively by integrating the responses across time windows corresponding to the sustained (Fig. 5B) and phasic (Fig. 5C) neuronal responses, followed by statistical analysis between conditions across individual trials. Both phasic and sustained CSD and MUA responses, to both stationary and moving stimuli, were significantly different from baseline ($t > 12.45$, $P < 10^{-5}$; all tests are two-tailed with ≈240–480 degrees of freedom), except for the sustained MUA responses, which were not significantly different ($t = .26$). All responses (phasic and sustained, MUA and CSD) were greater to moving than to stationary stimuli ($t > 9.22$, $P < 10^{-5}$), except for the sustained CSD responses, which were not significantly different ($t = .91$). Finally, all responses (phasic and sustained, MUA and CSD) were greater to coherently than to incoherently moving stimuli ($t > 4.79$, $P < 10^{-5}$), except for the sustained MUA responses, which were actually greater to the incoherently moving dots ($t = 21.15$, $P < 10^{-5}$).

DISCUSSION

Local cortical circuits processing coherent visual motion

The laminar distribution of population synaptic currents and action potentials were recorded from putative MT+ while the subject viewed the onset of a pattern of stationary dots that after a delay began to move, either coherently or incoherently. Moving stimuli were more effective in activating this structure than stationary stimuli, and coherent motion was more effective than incoherent.

An early sink in layer IV was evoked by coherently as well as incoherently moving visual stimuli. This is consistent with primate neuroanatomical studies showing that the projection from V1 and V2 to MT terminates predominately in layer IV [Rockland, 1989, 1995], as is typical for feedforward connections in the neocortex [Rockland and Pandya, 1979; Felleman and

Figure 4.

Responses in putative MT+ to coherent vs. incoherent motion. Current sources and sinks (indicated with black and white contour lines, respectively) are superimposed over a background showing the level of MUA activity (decreases indicated as blue and purple, increases as orange and red). MUA increases and decreases are also indicated by red and green contour lines, respectively. Cortical location (with more superficial lamina at top) is plotted against time relative to when the stationary dots (presented during the black bars) begin to move (red bars). **A.** The onset of coherent motion produces a large MUA increase as well as source-sink configurations in both deep (layers V–VI), as well as superficial (layer III) pyramidal laminae. The earliest response is in the deepest pyramidal layers, with MUA onset at about 90 ms and peak CSD response of about 1 $\mu A/mm^3$ at 150 ms. **B.** Incoherent motion onset produces a similar but much weaker and slightly delayed CSD and MUA response. **C.** Subtraction of the response to incoherent from that to coherent motion reveals the initially greater CSD and MUA in both superficial and deep pyramidal layers, followed by a greater decrease. **D.** Using a compressed time base, a phasic deep MUA and CSD response to stationary stimulus onset is seen. Stationary stimulus onset also evokes sustained rhythmic CSD in superficial layers without accompanying MUA. This superficial activity continues through the onset of motion (coherent and incoherent are combined in this panel). This overlap prevents clear interpretation of superficial CSD activity to visual motion. In deeper cortical laminae, the onset and offset of motion both evoke much larger CSD and MUA responses than does the onset of the stationary pattern. Responses are shown relative to a baseline prior to stimulus motion onset (−67 to 33 ms) in panels A–C or to a baseline prior to stationary stimulus onset (−1033 to −633 ms) in panel D, with zero time indicating motion onset. In all panels, for both CSD and MUA, thick contour lines indicate $P < 10^{-5}$ (uncorrected for multiple comparisons). For panels A, B and D, the first thin contour line indicates $P < 10^{-3}$ with additional thin contour lines at *t*-score increments of 1 (for MUA) or 2 (for CSD). In panel C, thin contour lines are at $P <$ 0.002, 0.001, 0.0001, and 0.000002.

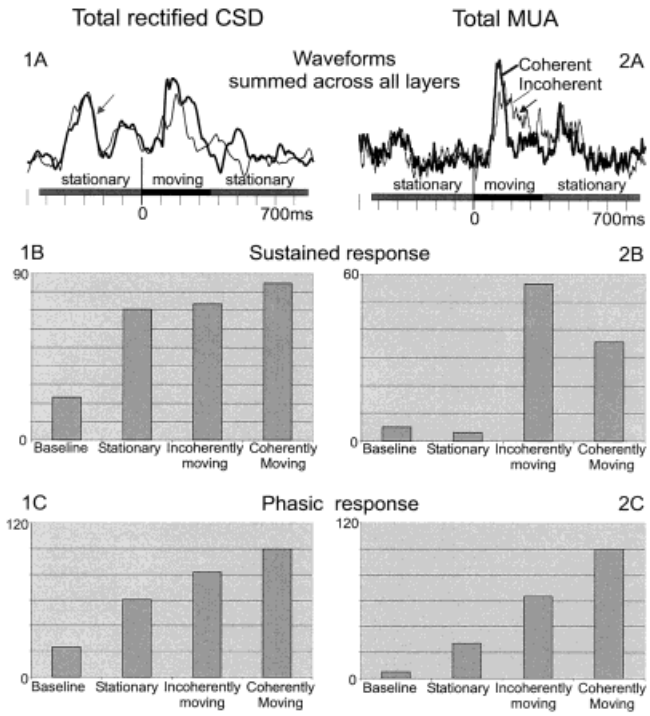

Figure 5.

Total estimated transcortical synaptic currents and action potentials. The left panels (**1A,B,C**) display the total CSD, as rectified and summed across the different cortical layers. The right panels (**2A,B,C**) display the total MUA, again summed across cortical layers. The top panels (1A,2A) show the waveforms calculated over the entire trial, including the prestimulus baseline, stationary visual stimuli, moving stimuli, and again stationary stimuli. The middle panels (1B,2B) show the total CSD and MUA integrated over long time windows chosen to encompass the entire neuronal responses, to stationary stimuli (90–583 ms after stationary stimulus onset) and coherently or incoherently moving stimuli (90–423 ms after motion onset) in comparison to the baseline (500–100 ms prior to stationary stimulus onset). The responses are divided by the duration of the integration window, and normalized to the phasic response to coherently moving stimuli. The bottom panels (1C,2C) show the total CSD and MUA integrated over time windows chosen to reflect the phasic neuronal responses to stationary and moving stimuli (90–180 or 90–160 ms after the respective stimulus onsets) in comparison to the same prestimulus baseline. The phasic reponses display the general effects predicted by the BOLD response in previous studies: a progressive increase from baseline, to stationary, to incoherently moving, to coherently moving stimuli. The sustained responses deviate from these predictions, as discussed in the text.

VanEssen, 1991]. An early deep pyramidal layer source was also noted, as has previously been found in laminar CSD/MUA recordings from macaque visual association cortex [Mehta et al., 2000]. This may correspond to the observation that the V1 projection to MT is not only to layer IV but also includes layer VI [Rockland, 1989].

The presence of a differentiated response in the deepest pyramids is of particular significance because the neocortex is generally organized such that the deep pyramids are the usual origin of long-range subcortical and cortico-cortical projections [Rockland and Pandya, 1979; Felleman and VanEssen, 1991]. From MT+, these fibers project to the superior colliculus, basal ganglia, thalamus, brainstem, and parieto-frontal occulomotor and visual attention areas, where they are thought to play a role in integrating optic flow with perceptual stabilization and oculomotor control [Ungerleider et al., 1984; Ungerleider and Desimone, 1986; Boussaoud et al., 1990]. Thus, the current results show that by ≈110 ms after motion onset, there is a strong output from MT+ indicating to distant target structures whether that motion is coherent.

The CSD/MUA response in the deep pyramidal layer is followed after ≈20 ms with a CSD/MUA response in the superficial pyramidal layer. These responses appeared to be linked, in that they covaried across conditions in latency and strength. This delayed coupling between deep and superficial pyramidal activity is consistent with numerous studies in animals that have identified a powerful excitatory local projection from deep to superficial pyramidal cells (see for example the laminar studies of rat sensory cortex by Sukov and Barth [1998]).

Following these phasic responses, moving stimuli evoke a sustained deep pyramidal CSD response that is larger to coherent motion, and a MUA response that is larger to incoherent. This dissociation could be explained by increased recurrent inhibition following the increased initial excitation evoked by coherent stimuli. A prominent feature of local intracortical circuitry is that the recurrent collaterals of pyramidal cells strongly activate inhibitory neurons, which then recurrently inhibit the pyramids [Berman et al., 1992].

The relatively short latencies recorded here correspond to previous observations of responses in the dorsal visual stream. Anatomical [Snowden et al., 1992; Anderson et al., 1998] and physiological [Maunsell et al., 1990; Sclar et al., 1990; Gegenfurtner et al., 1994] evidence in macaques suggests that motion-sensitive activation is projected from the magnocellular division of the lateral geniculate body to cells in layer IVB of area V1, which project directly to MT+ via rapid highly myelinated fibers [Rockland, 1989]. The lower layers of human MT+ are also myelinated [Clarke and Miklossy, 1990], and MT+ hemodynamic activation has high contrast–sensitivity and low chromatic-sensitivity, suggesting that the human MT+ re-

ceives motion-selective activation from V1 [Tootell et al., 1995]. Although MST follows MT in the dorsal visual processing stream [Ungerleider and Desimone, 1986; Boussaoud et al., 1990], the response latencies of MST neurons are about the same as those of MT neurons in macaques [Schmolesky et al., 1998]. In general, these latencies are quite short in comparison with the ventral stream pathway. In fact, laminar recordings in the macaque found that average response latencies from the region of MT+ were *shorter* than those from V1 [Schroeder et al., 1998]! In human extracranial EEG and MEG recordings, the earliest responses in V1 occur at a latency to peak of about 70 ms [Regan, 1989], and motion-sensitive components over MT+ occur with a peak latency of about 150 ms [Kuba and Kubova, 1992; Dale et al., 1996; Ahlfors et al., 1999; Nakamura and Ohtsuka, 1999], which correspond well with those observed in the current study.

It is noteworthy that the differentiation in the MUA responses to coherent vs. incoherent motion is visible at the onset of the response, and is significant shortly thereafter. This argues strongly against models wherein the selectivity for coherent motion arises from network interactions within MT+. In any case, these data show clearly that not only was the initial MUA increase stronger to coherent stimuli, the subsequent decrease (peaking about 70 ms after the excitatory peak) was also much stronger to coherent stimuli. This finding is in direct contradiction to the opponent inhibition feedback model, which predicts that the inhibition following the initial excitation should be larger to the *in*coherent stimuli.

Overall, the patterns of synaptic and unit activation observed here correspond to that expected from previous studies in animals, and thus confirms that these model studies are applicable to humans performing behavioral tasks. The current results are clearly limited because they are multiunit rather than based on an examination of individual neurons with previously identified receptive fields. Nonetheless, the current results describe with an unprecedented level of detail the synaptic and unit responses of MT+ neurons in the awake human to coherent and incoherent stimuli, and thus should provide data relevant to future theorizing.

Neural correlates of the BOLD response

These data also have implications for the relation between neuronal activity and the BOLD (blood oxygenation level dependent) response measured with fMRI. This is a crucial issue because although the BOLD response has been used extensively to noninvasively localize brain activation during behavioral tasks in humans, BOLD is a hemodynamic measure that has a delayed and indirect relation to the synaptic and neural activity that actually embodies ongoing information processing [Buxton et al., 1998]. In particular, there is no well-accepted quantitative model that calculates the BOLD response from detailed electrophysiological measurements and no empirical studies of that relationship for high-level cognitive tasks in people.

Because much of the metabolic effort in the brain goes toward restoring ionic balances disturbed by trans-synaptic current flows, it is possible that the hemodynamic response closely mirrors those flows [Frostig et al., 1990]. This hypothesis would predict a close correspondence between the behavioral response profiles of CSD (as reported here) with those found in previous fMRI/PET studies. Other studies have suggested that a linear relationship exists between unit activity recorded in macaques and the BOLD response measured in humans in the same or a similar task [e.g., Heeger et al., 1999]. Because unit activity arises from synaptic activity, these measures are usually coupled. However, high levels of synaptic activity without cell-firing may occur if there is simultaneous excitatory currents at distal dendrites and inhibition at proximal locations [e.g., Larkum et al., 1999].

Indeed, in the current study, both total synaptic activity (as estimated by CSD) and total neuronal firing (as estimated by MUA), strongly increased over baseline in response to moving visual stimuli and (at least acutely) in response to coherent vs. incoherent motion (Fig. 5), both cardinal properties of the BOLD response in MT+ [Tootell et al., 1995]. Furthermore, both MUA and CSD responded transiently to stationary stimulus onset and to the termination of visual motion, as has been reported for the BOLD response [Tootell et al., 1995].

However, important dissociations can also be found between the CSD or MUA responses and the BOLD responses reported in the literature to similar stimuli. For example, the total CSD was clearly greater to coherent than incoherent motion both acutely and over the entire stimulation period. In contrast, the initially greater increase of MUA to coherent stimuli was followed by a greater decrease beginning at ≈133 ms, possibly because of recurrent inhibition. This resulted in the total MUA actually being greater to *incoherent* stimuli when measured over the entire stimulus period (Fig. 5). This conclusion runs counter to that of Rees et al. [2000] who concluded that increasing the coherence of visual motion increased macaque MT

unit activity as well as the human MT+ BOLD response. Rees et al. [2000] used the macaque data of Britten et al. [1993] who quantified the responses of MT+ neurons that had been preselected to be responsive to random dot patterns in a directionally sensitive manner. They used a sharpened high-impedance microelectrode that was moved until a single cell was isolated. In contrast, the current study used a relatively large recording surface and sampled MUA at regular fixed intervals of 175μ across the cortical depth. In addition, we sampled only one cortical traverse, whereas Britten et al. (1993) sampled many. The sampling bias induced by these multiple factors is difficult to evaluate.

Although in this comparison of the sustained response to coherent vs. incoherent motion, CSD seems to track the BOLD response better than does MUA; the opposite pattern was observed for the overall sustained responses to stationary vs. moving stimuli, which MUA distinguished much more strongly than did CSD. Sustained MUA levels were over tenfold higher for moving than for stationary stimuli or baseline, which were about equal. In contrast, sustained CSD levels did not differ significantly between stationary and moving stimuli, although both were greater than baseline. It should be noted that in their acute responses, MUA and CSD behaved similarly, being greater to stationary stimuli than baseline, and greater to moving than stationary.

Thus, in both cases where the neuronal responses to stimulation parameters differed from what BOLD would predict, the divergence was observed only for the sustained measures, not for the acute response. This is unexpected because the BOLD response is thought to act like a low-pass filter on the metabolic demand [Buxton et al., 1998], and the BOLD responses to successive neuronal demands are thought to add linearly [Dale and Buckner, 1997]. The net effect of these two properties should be that the BOLD response would track the integrated neuronal activity level over the entire stimulation period rather than the initial phasic response.

In the two critical cases where the tracking between neuronal and BOLD responses are reversed from that expected there are particular explanations that may not generalize to other situations. Specifically, stationary stimuli evoked large sustained CSD oscillations in the superficial cortical layers without inducing significant MUA and possibly without entailing increased metabolic demand. Similarly, the net decrease in MUA to coherent vs. incoherent motion at longer latencies appeared to be caused by recurrent inhibition, i.e., sustained excitatory drive accompanied by inhibitory currents at the soma that effectively decrease cell firing. An apparently similar phenomenon was reported by Ackermann et al. [1984] who found that metabolism (measured with 2DG) increases in the deafferented hippocampus when the fornix is stimulated, producing brief excitation followed by a long and profound active inhibition.

Thus, in this study, special factors seem to render the later CSD and MUA levels less reliable than the initial for predicting the BOLD response. It is unclear from this initial study whether these factors will also be operative in other cortical areas or behavioral tasks. Theoretical physiological analysis suggests that many dissociations are possible between population synaptic activity, unit activity, and the BOLD response. If the findings of this study generalize, then it may be found that the initial neuronal response is more representative of the metabolic demand than is the sustained response. Experimental studies in the primary sensory cortices of animals have emphasized the relationship of the initial layer IV neuronal response to the overall hemodynamic response, and thus are consistent with this interpretation [e.g., Woolsey et al., 1996].

CONCLUSION

Population synaptic and unit activity in putative human MT+ respond strongly and differentially to moving vs. stationary visual stimuli, and especially to coherent motion. The differential response is especially early and strong in the layers that project to other visual motion and occulomotor areas. The differential response to coherent vs. incoherent motion is present from the onset of the response, and thus does not depend on secondary processing by interneurons. However, the MUA/CSD patterns suggest that recurrent inhibition may play an important role in mediating tonic differences between such stimuli. In addition, the current results emphasize the complexity of the relationship between neural activity and the hemodynamic response and the importance of further detailed studies with simultaneous metabolic and electrophysiological measures. The potential variability in this relationship requires that conclusions from model studies be validated in humans performing cognitive tasks.

ACKNOWLEDGMENTS

We thank L. Shuer and M. Reisinger for clinical collaboration, A. Dale and J. Mendola for scientific collaboration, and B. Harris for histology.

REFERENCES

Ackermann RF, Finch DM, Babb TL, Engel J Jr. (1984): Increased glucose metabolism during long-duration recurrent inhibition of hippocampal pyramidal cells. J Neurosci 4:251–264.

Ahlfors SP, Simpson GV, Dale AM, Belliveau JW, Liu AK, Korvenoja A, Virtanen J, Huotilainen M, Tootell RB, Aronen HJ, Ilmoniemi RJ (1999): Spatiotemporal activity of a cortical network for processing visual motion revealed by MEG and fMRI. J Neurophysiol 82:2545–2555.

Andersen RA, Shenoy KV, Crowell JA, Bradley DC (2000) Neural mechanisms for self-motion perception in area MST. Int Rev Neurobiol 44:219–233.

Anderson JC, Binzegger T, Martin KA, Rockland KS (1998): The connection from cortical area V1 to V5: a light and electron microscopic study. J Neurosci 18:10525–10540.

Berman NJ, Douglas RJ, Martin KA (1992): GABA-mediated inhibition in the neural networks of visual cortex. Prog Brain Res 90:443–476.

Boussaoud DB, Ungerleider LG, Desimone R (1990): Pathways for motion analysis: cortical connections of the medial superior temporal and fundus of the superior temporal visual areas in the macaque. J Comp Neurol 296:462–495.

Bradley DC, Andersen RA (1998): Center-surround antagonism based on disparity in primate area MT. J Neurosci 18:7552–7565.

Britten KH, Shadlen MN, Newsome WT, Movshon JA (1993): Responses of neurons in macaque MT to stochastic motion signals. Vis Neurosci 10:1157–1169.

Buxton RB, Wong EC, Frank LR (1998): Dynamics of blood flow and oxygenation changes during brain activation: the balloon model. Magn Reson Med 39:855–864.

Clarke S, Miklossy J (1990): Occipital cortex in man. Organisation of callosal connections, related myelo- and cytoarchitecture, and putative boundaries of functional visual areas. J Comp Neurol 298:188–214.

Dale AM, Ahlfors SP, Aronen HJ, Belliveau JW, Huotilainen M, Ilmoniemi RJ, Kennedy WA, Korvenoja A, Liu AK, Reppas JB, Rosen BR, Sereno MI, Simpson GV, Standertskjold-Nordenstam C-G, Tootell RBH, Virtanen J (1996): Spatiotemporal imaging of motion processing in human visual cortex. Neuroimage 3:S359.

Dale AM, Buckner RL (1997): Selective averaging of rapidly presented individual trials using fMRI. Hum Brain Mapp 5:329–340.

Duffy CJ, Wurtz RH (1991): Sensitivity of MST neurons to optic flow stimuli. I. A continuum of response selectivity to large-field stimuli. J Neurophysiol 65:1329–1345.

Felleman DJ, VanEssen DC (1991): Distributed hierarchical processing in the primate cerebral cortex. Cereb Cortex 1:1–47.

Frostig RD, Lieke EE, Ts'o DY, Grinvald A (1990): Cortical functional architecture and local coupling between neuronal activity and the microcirculation revealed by in vivo high-resolution optical imaging of intrinsic signals. Proc Natl Acad Sci U S A 87:6082–6086.

Geesaman BJ, Born RT, Andersen RA, Tootell RB (1997): Maps of complex motion selectivity in the superior temporal cortex of the alert macaque monkey: a double-label 2-deoxyglucose study. Cereb Cortex 7:749–757.

Gegenfurtner KR, Kiper DC, Beusmans JM, Carandini M, Zaidi Q, Movshon JA (1994): Chromatic properties of neurons in macaque MT. Vis Neurosci 11:455–466.

Graziano MS, Andersen RA, Snowden RJ (1994): Tuning of MST neurons to spiral motions. J Neurosci 14:54–67.

Grover FS, Buchwald JS. 1970. Correlation of cell size with amplitude of background fast activity in specific brain nuclei. J Neurophysiol 33:160–171.

Halgren E, Babb TL, Crandall PH (1977): Responses of human limbic neurons to induced changes in blood gases. Brain Res 132:43–63.

Heeger DJ, Boynton GM, Demb JB, Seidemann E, Newsome WT (1999): Motion opponency in visual cortex. J Neurosci 19:7162–7174.

Kuba M, Kubova Z (1992): Visual evoked potentials specific for motion onset. Doc Ophthalmol 80:83–89.

Lagae L, Maes H, Raiguel S, Xiao DK, Orban GA (1994): Responses of macaque STS neurons to optic flow components: a comparison of areas MT and MST. J Neurophysiol 71:1597–1626.

Lappe M, Bremmer F, Pekel M, Thiele A, Hoffmann KP (1996): Optic flow processing in monkey STS: a theoretical and experimental approach. J Neurosci 16:6265–6285.

Lappe M, Duffy CJ (1999): Optic flow illusion and single neuron behaviour reconciled by a population model. Eur J Neurosci 11:2323–2331.

Larkum ME, Zhu JJ, Sakmann B (1999): A new cellular mechanism for coupling inputs arriving at different cortical layers. Nature 398:338–341.

Legatt AD, Arezzo JC, Vaughan HGJ (1980): Averaged multiple unit activity as an estimate of phasic changes in local neuronal activity: effects of volume-conducted potentials. J Neurosci Meth 2:203–217.

Maunsell JH, Nealey TA, DePriest DD (1990): Magnocellular and parvocellular contributions to responses in the middle temporal visual area (MT) of the macaque monkey. J Neurosci 10:3323–3334.

Maunsell JH, VanEssen DC (1983): Functional properties of neurons in middle temporal visual area of the macaque monkey. I. Selectivity for stimulus direction, speed, and orientation. J Neurophysiol 49:1127–1147.

Mehta AD, Ulbert I, Schroeder CE (2000): Intermodal selective attention in monkeys. II. Physiological mechanisms of modulation. Cereb Cortex 10:359–370.

Mitzdorf U (1985): Current source-density method and application in cat cerebral cortex: investigation of evoked potentials and EEG phenomena. Physiol Rev 65:37–100.

Nakamura Y, Ohtsuka K (1999): Topographical analysis of motion-triggered visual-evoked potentials in man. Jpn J Ophthalmol 43:36–43.

Nicholson C, Freeman JA. 1975. Theory of current source density analysis and determination of the conductivity tensor for anuran cerebellum. J Neurophysiol 38:356–368.

Perrone JA, Stone LS (1998): Emulating the visual receptive-field properties of MST neurons with a template model of heading estimation. J Neurosci 18:5958–5975.

Rappelsberger P, Pockberger H, Petsche H (1981): Current source density analysis: methods and application to simultaneously recorded field potentials of the rabbit's visual cortex. Pflugers Arch 389:159–170.

Regan D (1989): Human brain electrophysiology. New York: Elsevier.

Rockland KS (1989): Bistratified distribution of terminal arbors of individual axons projecting from area V1 to middle temporal area (MT) in the macaque monkey. Vis Neurosci 3:155–170.

Rockland KS (1995): Morphology of individual axons projecting from area V2 to MT in the macaque. J Comp Neurol 355:15–26.

Rockland KS, Pandya DN (1979): Laminar origins and terminations of cortical connections of the occipital lobe in the rhesus monkey. Brain Res 179:3–20.

Schmolesky MT, Wang Y, Hanes DP, Thompson KG, Leutgeb S, Schall JD, Leventhal AG (1998): Signal timing across the macaque visual system. J Neurophysiol 79:3272–3278.

Schroeder CE, Mehta AD, Givre SJ (1998): A spatiotemporal profile of visual system activation revealed by current source density analysis in the awake macaque. Cereb Cortex 8:575–592.

Schroeder CE, Steinschneider M, Javitt DC, Tenke CE, Givre SJ, Mehta AD, Simpson GV, Arezzo JC, Vaughan HG Jr. (1995): Localization of ERP generators and identification of underlying neural processes. Electroencephalogr Clin Neurophysiol Suppl 44:55–75.

Sclar G, Maunsell JHR, Lennie P (1990): Coding of image contrast in central visual pathways of the macaque monkey. Vis Res 30:1–10.

Snowden RJ, Treue S, Andersen RA (1992): The response of neurons in areas V1 and MT of the alert rhesus monkey to moving random dot patterns. Exp Brain Res 88:389–400.

Sukov W, Barth DS (1998): Three-dimensional analysis of spontaneous and thalamically evoked gamma oscillations in auditory cortex. J Neurophysiol 79:2875–2884.

Talairach J, Tournoux P (1988): Co-planar stereotaxic atlas of the human brain. New York: Thieme.

Tanaka K, Fukada Y, Saito HA (1989): Underlying mechanisms of the response specificity of expansion/contraction and rotation cells in the dorsal part of the medial superior temporal area of the macaque monkey. J Neurophysiol 62:642–656.

Tanaka K, Hikosaka K, Saito H, Yukie M, Fukada Y, Iwai E (1986): Analysis of local and wide-field movements in the superior temporal visual areas of the macaque monkey. J Neurosci 6:134–144.

Tootell RBH, Reppas JB, Kwong KK, Malach R, Born RT, Brady TJ, Rosen BR, Belliveau JW (1995): Functional analysis of human MT and related visual areas using magnetic resonance imaging. J Neurosci 15:3215–3230.

Ulbert I, Halgren E, Heit G, Karmos G (2001): Multiple microelectrode-recording system for human intracortical applications. J Neurosci Meth 106:69–79.

Ungerleider L, Desimone R, Galkin TW, Mishkin M (1984): Subcortical projections of area MT in the macaque. J Comp Neurol 223:368–386.

Ungerleider LG, Desimone R (1986): Cortical connections of visual area MT in the macaque. J Comp Neurol 248:190–222.

Vaknin G, DiScenna PG, Teyler TJ (1988): A method for calculating current source density (CSD) analysis without restoring sites outside the sampling volume. J Neurosci Meth 24:131–135.

Watson JD, Myers R, Frackowiak RSJ, Hajnal JV, Woods RP, Mazziotta JC, Shipp S, Zeki S (1993): Area V5 of the human brain: evidence from a combined study using positron emission tomography and magnetic resonance imaging. Cereb Cortex 3:79–94.

Woolsey TA, Rovainen CM, Cox SB, Henegar MH, Liang GE, Liu D, Moskalenko Y, Sui J, Wei L (1996): Neuronal units linked to microvascular modules in cerebral cortex: response elements for imaging the brain. Cereb Cortex 6:647–660.